HHS Public Access

Author manuscript

J Med Chem. Author manuscript; available in PMC 2023 February 24.

Published in final edited form as:

J Med Chem. 2022 February 24; 65(4): 3218–3228. doi:10.1021/acs.jmedchem.1c01709.

Thieno[2,3-*d*]pyrimidine-based Positive Allosteric Modulators of Human MAS-Related G Protein-Coupled Receptor X1 (MRGPRX1)

Ilyas Berhane[†,‡], **Niyada Hin**[†], **Ajit G. Thomas**[†], **Qian Huang**[§], **Chi Zhang**[§], **Vijayabhaskar Veeravalli**[†,‡], **Ying Wu**[†], **Justin Ng**[†], **Jesse Alt**[†], **Camilo Rojas**[†], **Hiroe Hihara**[¶], **Mika Aoki**[¶], **Kyoko Yoshizawa**[¶], **Tomoki Nishioka**[¶], **Shuichi Suzuki**[¶], **Shao-Qiu He**[§], **Qi Peng**[#], **Yun Guan**[§], **Xinzhong Dong**[#], **Srinivasa N. Raja**[§], **Barbara S. Slusher**[†,‡,#], **Rana Rais**[†,‡], **Takashi Tsukamoto**[†,‡]

[†]Johns Hopkins Drug Discovery, Johns Hopkins University, Baltimore, MD 21205, USA

[‡]Department of Neurology, Johns Hopkins University, Baltimore, MD 21205, USA

[§]Department of Anesthesiology and Critical Care Medicine, Johns Hopkins University, Baltimore, MD 21205, USA

Corresponding Authors: Rana Rais – Johns Hopkins Drug Discovery, Neurology, and Pharmacology, Johns Hopkins University, Baltimore, Maryland 21205, United States; rrais2@jhmi.edu, Takashi Tsukamoto – Johns Hopkins Drug Discovery, Neurology, and Pharmacology, Johns Hopkins University, Baltimore, Maryland 21205, United States; ttsukamoto@jhmi.edu.

Ilyas Berhane – Johns Hopkins Drug Discovery and Neurology, Johns Hopkins University, Baltimore, Maryland 21205, United States

Niyada Hin – Johns Hopkins Drug Discovery, Johns Hopkins University, Baltimore, Maryland 21205, United States

Ajit G. Thomas – Johns Hopkins Drug Discovery, Johns Hopkins University, Baltimore, Maryland 21205, United States

Qian Huang – Anesthesiology and Critical Care Medicine, Johns Hopkins University, Baltimore, Maryland, 21205, United States

Chi Zhang – Anesthesiology and Critical Care Medicine, Johns Hopkins University, Baltimore, Maryland, 21205, United States

Vijayabhaskar Veeravalli – Johns Hopkins Drug Discovery and Neurology, Johns Hopkins University, Baltimore, Maryland 21205, United States

Ying Wu – Johns Hopkins Drug Discovery, Johns Hopkins University, Baltimore, Maryland 21205, United States

Justin Ng – Johns Hopkins Drug Discovery, Johns Hopkins University, Baltimore, Maryland 21205, United States

Jesse Alt – Johns Hopkins Drug Discovery, Johns Hopkins University, Baltimore, Maryland 21205, United States

Camilo Rojas – Johns Hopkins Drug Discovery and Molecular and Comparative Pathobiology, Johns Hopkins University, Baltimore, Maryland 21205, United States

Hiroe Hihara – Tsukuba Research Laboratories, Eisai Co., Ltd., Tsukuba, Ibaraki 300-2635, Japan

Mika Aoki – Tsukuba Research Laboratories, Eisai Co., Ltd., Tsukuba, Ibaraki 300-2635, Japan

Kyoko Yoshizawa – Tsukuba Research Laboratories, Eisai Co., Ltd., Tsukuba, Ibaraki 300-2635, Japan

Tomoki Nishioka – Tsukuba Research Laboratories, Eisai Co., Ltd., Tsukuba, Ibaraki 300-2635, Japan

Shuichi Suzuki – Tsukuba Research Laboratories, Eisai Co., Ltd., Tsukuba, Ibaraki 300-2635, Japan

Shao-Qiu He – Anesthesiology and Critical Care Medicine, Johns Hopkins University, Baltimore, Maryland, 21205, United States

Qi Peng – Solomon H. Snyder Department of Neuroscience, Johns Hopkins University, Baltimore, Maryland, 21205, United States

Yun Guan – Anesthesiology and Critical Care Medicine and Neurological Surgery, Johns Hopkins University, Baltimore, Maryland, 21205, United States

Xinzhong Dong – Solomon H. Snyder Department of Neuroscience, Johns Hopkins University, Baltimore, Maryland, 21205, United State

Srinivasa N. Raja – Anesthesiology and Critical Care Medicine, Johns Hopkins University, Baltimore, Maryland, 21205, United States

Barbara S. Slusher – Johns Hopkins Drug Discovery, Neurology, Psychiatry and Behavioral Sciences, Pharmacology, Neuroscience, Medicine, and Oncology, Johns Hopkins University, Baltimore, Maryland 21205, United States;

Authors Contributions

All authors have contributed to the work and have given approval to the final version of the manuscript.

Supporting Information

The Supporting Information is available free of charge at https://pubs.acs.org/doi/10.1021/acs.jmedchem.1c01709.

^{1}H and ^{13}C spectra of the final compounds, *in vitro* selectivity profile of compound **1t**, and behavioral effects of compound **1t** in naive MRGPRX1 mice (PDF)

Molecular formula strings (CSV)

The authors declare no competing financial interest.

[#]Solomon H. Snyder Department of Neuroscience, Johns Hopkins University, Baltimore, MD 21205, USA

[¶]Tsukuba Research Laboratories, Eisai Co., Ltd., Tsukuba, Ibaraki 300-2635, Japan

Abstract

Mas-related G protein-coupled receptor X1 (MRGPRX1) is a human sensory neuron-specific receptor and potential target for the treatment of pain. Positive allosteric modulators (PAMs) of MRGPRX1 have the potential to preferentially activate the receptors at the central terminals of primary sensory neurons and minimize itch side effects caused by peripheral activation. Using a high-throughput screening (HTS) hit, a series of thieno[2,3-*d*]pyrimidine-based molecules were synthesized and evaluated as human MRGPRX1 PAMs in HEK293 cells stably transfected with human MrgprX1 gene. An iterative process to improve potency and metabolic stability led to the discovery of orally available 6-(tert-butyl)-5-(3,4-dichlorophenyl)-4-(2-(trifluoromethoxy)phenoxy)thieno[2,3-*d*]pyrimidine (**1t**), which can be distributed to the spinal cord, the presumed site of action, following oral administration. In a neuropathic pain model induced by sciatic nerve chronic constriction injury (CCI), compound **1t** (100 mg/kg, po) reduced behavioral heat hypersensitivity in humanized MRGPRX1 mice, demonstrating the therapeutic potential of MRGPRX1 PAMs in treating neuropathic pain.

Graphical Abstract

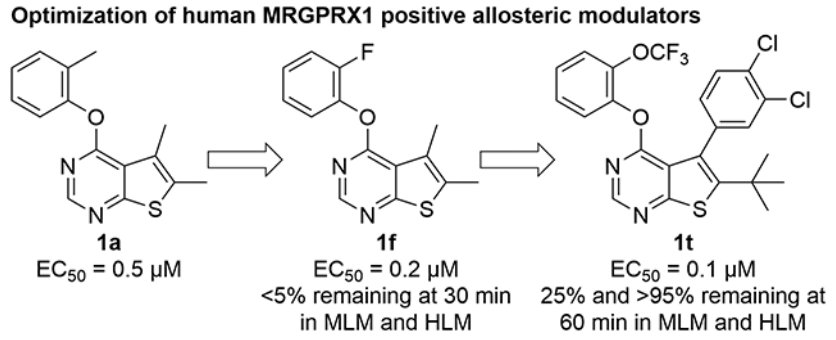

INTRODUCTION

Mas-related G protein-coupled receptor X1 (MRGPRX1) is expressed specifically in the small diameter dorsal root ganglion (DRG) sensory neurons and is implicated in the modulation of nociception.[1] MRGPRX1 has gained increased interest as a promising therapeutic target partly based on the analgesic effects of BAM8–22 (Figure 1),[2] a proteolytic product derived from proenkephalin A with full agonist activity at human MRGPRX1 and its closest rodent orthologues, mouse MRGPRC11 and rat MRGPRC.[3] DRG sensory neurons have both centrally and peripherally projecting axons. The analgesic effects of MRGPRX1 agonists are thought to be partially mediated by downstream inhibition of N-type calcium channels resulting in reduced synaptic inputs to the spinal cord dorsal horn neurons.[4] On the other hand, activation of peripheral MRGPRX1 localized in nerve terminals in the skin may generate an itch sensation.[5] These dual effects produced by direct activation of MRGPRX1 at the central and peripheral terminals of DRG neurons

may limit the therapeutic utility of small molecule orthosteric MRGPRX1 agonists[6, 7] for systemic treatment. Interestingly, BAM22, another endogenous peptide-based MRGPRX1 agonist, was found to be upregulated at spinal dorsal horn during persistent pain after nerve injury or tissue inflammation, while it was undetectable in the skin.[8] These findings have presented a unique therapeutic opportunity for positive allosteric modulators (PAMs) of MRGPRX1, which can potentiate the agonist effects of the endogenous agonist at the central terminals of sensory neurons without activating peripheral MRGPRX1, thus minimizing itch side effects.

2-[(Cyclopropylsulfonyl)amino]-*N*-(2-ethoxyphenyl)benzamide, also known as ML382, is a prototype MRGPRX1 PAM identified by the Molecular Libraries Probe Production Centers Network (MLPCN).[9] ML382 was found to inhibit pain hypersensitivity after injury following intrathecal injection, and systemic administration of ML382 did not elicit itch side effects.[8] These findings confirm the presence of endogenous MRGPRX1 agonists in the spinal cord during persistent pain conditions and demonstrate the therapeutic potential of MRGPRX1 PAMs as novel analgesic agents devoid of the peripheral itch side effects. However, ML382 produces analgesic effects only when injected intrathecally presumably due to its poor distribution to the spinal cord, limiting its therapeutic utility in treating chronic neuropathic pain. This prompted us to explore structurally distinct MRGPRX1 PAMs with improved pharmacokinetics properties and in vivo analgesic efficacy following oral administration.

To this end, we conducted high throughput screening of Eisai's compound library in HEK293 cells stably transfected with human MRGPRX1 by using FLIPR Calcium 4 Assay Kit (Molecular Devices) to measure intracellular calcium responses.[10] We identified 5,6-dimethyl-4-(*o*-tolyloxy)thieno[2,3-*d*]pyrimidine **1a** as a potent MRGPRX1 PAM with an EC_{50} value of 0.5 μM. Although compound **1a** is less potent than ML382, its lack of a hydrogen bond donor prompted us to use this hit compound as a molecular template in an attempt to identity MRGPRX1 PAMs with improved pharmacokinetics properties. Here, we describe the design, synthesis, and structure−activity relationships (SAR) of a new series of human MRGPRX1 PAMs using compound **1a** as a molecular template. Our optimization efforts aimed at improving not only MRGPRX1 PAM potency but also metabolic stability led to the discovery of an orally available MRGPRX1 PAM, potentially valuable as a new lead for treating neuropathic pain.

CHEMISTRY

Compounds **1a-p** were synthesized by reacting 4-chloro-thieno[2,3-*d*]pyrimidines **2a-f** with various phenols pretreated with NaH (Scheme 1).

Compound **1q** was synthesized in three steps starting with a one-pot synthesis of thieno[2,3-*d*]pyrimidin-4-ol **4** via Gewald reaction.[11] Compound **4** was subsequently converted to 4-chloro derivative **5** by treating with phosphoryl chloride. Nucleophilic substitution with 2-fluorophenol afforded the desired product **1q**.

Although the synthetic route developed for compound **1q** (Scheme 2) described above takes only three steps to the desired product, it suffered from the poor yield in the first step involving the four-component reaction, presumably due to the steric hindrance by the *tert*-butyl group in starting material **3**. This prompted us to explore alternative routes to compounds **1r-t** containing a *tert*-butyl group at the 6-position. As shown in scheme 3, 6-(*tert*-butyl)-4-chlorothieno[2,3-*d*]pyrimidine **2f** was first converted into the 6-methoxy derivative **6**. Compound **6** was brominated at its 5-position by NBS to give compound **7**. Suzuki coupling of compound **7** with aryl boronic acids gave compounds **8a-b**. After converting **8a-b** to 4-chloro derivative **10a-b**, the desired product **1r-t** was obtained by reacting them with either 2-fluorophenol or 2-trifluoromethoxyphenol.

RESULTS AND DISCUSSION

In vitro experiments measuring PAM activity at MRGPRX1 were performed with a FLIPR assay using HEK293 cells stably transfected with MRGPRX1 in the presence of EC_{20} (5–15 nM) of BAM8–22, a MRGPRX1 agonist devoid of opioid receptor affinity displayed by BAM22. The results are summarized in Table 1. All of the compounds with a submicromolar EC_{50} value displayed E_{max} ≥95% relative to the maximum response achieved by BAM8–22 alone. It should be noted that compound **1b** was also identified as an active allosteric MRGPRX1 activator by the NIH Molecular Libraries Probe Centers Network (MLPCN).[12] In our assay, compound **1b** displayed 20-fold lower potency compared to compound **1a,** indicating an important role played by the 5- and 6-methyl groups of **1a** in the PAM potency. Thus, we tested 5,6-dimethylthieno[2,3-*d*]pyrimidine derivatives **1c-k** possessing various phenoxy groups at the 4-position. Compound **1c** containing an unsubstituted phenoxy group showed 4-fold loss in potency compared to **1b**. *m*-Tolyloxy and *p*-tolyloxy derivatives **1d** and **1e** displayed substantially lower potency. We also explored fluoro and trifluoromethyl substitutions at the 4-phenoxy group in a systematic manner (compounds **1f-k**). As observed with methyl substitutions, ortho-substituted derivatives **1f** and **1i** exhibited greater potency than *meta*- and *para*-substituted derivatives **1g-h** and **1j-k**. Among these, compound **1f** containing a 2-fluorophenoxy group at the 4-position showed the most potent PAM activity.

In the subsequent set of compounds, we retained the 2-fluorophenoxy group at the 4-position and modified the 5- and 6-positions of the thieno[2,3-*d*]pyrimidine ring. Compound **1l** unsubstituted at the 5- and 6-positions showed much weaker potency. This is consistent with the substantial loss of potency observed in compound **1b** as compared to **1c**. The removal of one methyl group either from 5- or 6-position from **1a** also resulted in loss of potency as seen in compounds **1m** and **1n**. Replacement of the 5-methyl group with a trifluoromethyl group (compound **1o**) did not improve the potency either. Interestingly, introduction of a *tert*-butyl group into the 6-position (compounds **1p-r**) led to submicromolar potency.

In the last stage, we incorporated a 2-(trifluoromethyl)phenoxy group into the 4-position of the 6-(*tert*-butyl)thieno[2,3-*d*]pyrimidine scaffold as seen in compounds **1s** and **1t**. Compound **1t** represents one of the most potent MRGPRX1 PAMs within this series. We

also confirmed that compound **1t** has no intrinsic agonist activity at concentrations up to 100 μM in the absence of BAM8–22 (Supporting information Figure S1).

Structural optimization detailed above was guided by not only PAM potency but also metabolic stability. Table 2 summarizes the metabolic stability (%remaining after 30 and 60 min of incubation) of selected compounds in mouse and human liver microsomes. Compound **1f** was extensively metabolized within 30 min in both human and mouse microsomes. Notably, the loss of the parent compound was only observed in the presence of NADPH, suggesting CYP450-mediated oxidation involved in the metabolism of **1f**. Metabolite identification was attempted for compound **1f** using HR-MS analysis. A sample from compound **1f** exposed to human liver microsomes for 60 min exhibited a new peak representing [MH^+ + 16] (291.0612), suggesting an insertion of an oxygen atom into the parent compound (Figure 2). Fragmentation of the Phase I metabolite using MS/MS spectroscopy showed a major peak for a fragment at 170.0256, corresponding to the oxidized thiophene moiety (Figure 2), indicating that the CYP450-mediated oxidation was primarily taking place on the thieno[2,3-*d*]pyrimidine moiety of compound **1f**.

Compound **1o** was designed to make the thieno[2,3-d]pyrimidine ring electron-deficient by the electron-withdrawing effects of the 5-trifluoromethyl group. Although it showed slightly better stability in human liver microsomes, it failed to show any improvement over compound **1f** in mouse liver microsomes. Interestingly, compounds **1p-r** possessing a tert-butyl group at the 6-position showed substantially improved stability in human liver microsomes, presumably by protecting the thieno portion from oxidation. As seen with compound **1f**, however, these three compounds were extensively metabolized within a period of 30 min in mouse liver microsomes. Given these species-dependent metabolic stability data, it is conceivable that another site is being metabolized in mouse liver microsomes. Indeed, upon incorporation of a 2-(trifluoromethoxy)phenoxy group into the 4-position (compound **1s**), a slight improvement in stability was achieved against mouse liver microsomes. It should be also noted that compound **1s** was completely stable in human liver microsomes. Finally, compound **1t**, in which a 3,4-dichlorophenyl is introduced into the 5-position, showed substantial improvement in stability against mouse liver microsomes with 25% remaining at 60 min.

Given its potent PAM activity and good metabolic stability, we selected compound **1t** for in vivo pharmacokinetics studies in mice. In addition to plasma and brain levels, we measured drug levels in spinal cord (Figure 3), which is the putative site of action for MRGPRX1 PAMs to attenuate spinal nociceptive transmission. As shown in Table 3, substantial levels of **1t** were detected in plasma (C_{max} = 38.98 ± 5.06 nmol/mL; $AUC_{0\text{-last}}$ = 108.53 ± 1.18 nmol*h/mL) following oral administration (100 mg/kg). In contrast, its distribution to the brain was substantially restricted. Compound **1t**, however, was distributed to the spinal cord (C_{max} = 4.60 ± 0.60 nmol/mL; $AUC_{0\text{-last}}$ = 13.79 ± 0.14 nmol*h/mL) with a spinal cord-to-plasma ratio of 0.13. While C_{max} in the spinal cord is more than 40-fold greater than the EC_{50} value of compound **1t**, additional studies will be required to determine the precise PK/PD relationship, including evaluation of dose-response and quantification of unbound drug concentrations in the spinal cord tissues.

To assess its selectivity as a PAM, compound **1t** was tested in HEK293 cells stably expressing MRGPRX2 in the presence of EC_{20} concentration of C48/80,[13] a known MRGPRX2 orthosteric agonist, using Fluo-4 AM-based calcium detection assay (Supporting Information Figure S2). Compound **1t** showed no MRGPRX2 PAM activity at 5 μM, indicating at least 50-fold selectivity for MRGPRX1. Subsequently, a broader off-target activity profile of compound **1t** was evaluated by screening against a panel of 44 selected targets (Eurofins Cerep SafetyScreen 44) recommended by major pharmaceutical companies.[14] At 10 μM, compound **1t** was found to inhibit 5 targets (Supporting Information Table S1) by more than 50% (50−64%) including hERG channel. Although these off-target activities were detected at a concentration 100-fold greater than its EC_{50} value for MRGPRX1, future structural optimization efforts should aim to improve not only MRGPRX1 PAM potency but also selectivity over these targets.

To examine if compound **1t** elicits any adverse effect, spontaneous behaviors were video-recorded during 0–1 hour post-drug in awake, free-moving humanized MRGPRX1 mice, in which human MRGPRX1 is specifically expressed in nociceptive DRG neurons and replacing the murine homolog, MrgprC11.[8] Compared to vehicle, compound **1t** at this oral dose (100 mg/kg) caused no overt adverse effects including itch side effects as evident from the lack of spontaneous scratch bouts (Supporting Information Table S3). In the open field test, neither compound **1t** (100 mg/kg, po) nor vehicle significantly impaired exploratory performance in naïve MRGPRX1 mice as compared to pre-drug (Supporting Information Figure S3A–E). Furthermore, naïve MRGPRX1 mice treated with compound **1t** (100 mg/kg, po) showed no difference in performance on the rotarod test when compared to vehicle-treated group and pre-treatment values (Supporting Information Figure S3F). Collectively, no signs of acute toxicity were observed after oral administration of compound **1t** (100 mg/kg) in naïve MRGPRX1 mice, presumably due to its limited penetration to the brain and/or sensory neuron specific expression of MRGPRX1.

Compound **1t** was subsequently tested for its pain inhibitory effects *in vivo* following oral administration (100 mg/kg, po) in the sciatic nerve chronic constriction injury (CCI) model of neuropathic pain[15] using humanized MRGPRX1 mice. As shown in Figure 4, sciatic nerve CCI decreased paw withdrawal latency (PWL) to radiant heat stimuli in the hind paw (left) ipsilateral to the injury on days 12 and 26 post-injury, as compared to pre-injury level, suggesting heat hypersensitivity. The contralateral (right) PWL was not significantly changed after injury. Importantly, compound **1t** (100 mg/kg, po), but not vehicle, significantly increased ipsilateral PWLs from pre-drug level at 1 and 2 hours post-drug on day 12 (Figure 4A) and at 2 hours post-drug on day 26 post-injury (Figure 4B). There was no significant change of PWLs on the contralateral hind paw after drug treatment.

CONCLUSIONS

Chronic pain treatment remains a major medical challenge. There is a critical unmet medical need for new chronic pain therapies devoid of abuse potential and adverse effects. Restricted expression of human MRGPRX1 in primary nociceptive neurons provides a unique opportunity to develop analgesic agents targeting this receptor. The allosteric potentiation of MRGPRX1 appears to be a particularly attractive approach given the preferential

upregulation of endogenous MRGPRX1 agonists at the central terminals of primary sensory neurons, eliminating the possibility of itch side effects mediated by peripheral receptors. Using a thieno[2,3-*d*]pyrimidine-based hit compound **1a** identified from our HTS efforts as a molecular template, systematic structural optimization was carried out in an attempt to improve potency and pharmacokinetics properties. As described in this paper, our iterative efforts led to the discovery of more potent MRGPRX1 PAM **1t** with improved metabolic stability and good oral bioavailability, making it suitable for chronic treatment. As a proof of principle, our results with compound **1t** in a well-established neuropathic pain model represents the first report of *in vivo* efficacy achieved by an orally administered MRGPRX1 modulator in humanized MRGPRX1 mice. Studies are currently underway to not only further characterize compound **1t** as an analgesic agent but also identify more potent MRGPRX1 PAMs using compound **1t** as a new molecular template.

EXPERIMENTAL SECTION

General.

All solvents were reagent grade or HPLC grade. Unless otherwise noted, all materials were obtained from commercial suppliers and used without further purification. Melting points were obtained on a Mel-Temp apparatus and are uncorrected. ^{1}H NMR spectra were recorded at 400 or 500 MHz. ^{13}C NMR spectra were recorded at 101 or 125 MHz. The HPLC solvent system consisted of deionized water and acetonitrile, both containing 0.1% formic acid. Preparative HPLC purification was performed on an Agilent 1200 series HPLC system equipped with an Agilent G1315D DAD detector using a Phenomenex Luna 5 μm C18 column (21.2 mm × 250 mm, 5 μm). Analytical HPLC was performed on an Agilent 1200 series HPLC system equipped with an Agilent G1315D DAD detector (detection at 220 nm) and an Agilent 6120 quadrupole MS detector. Unless otherwise specified, the analytical HPLC conditions involve 20% acetonitrile/80% water for 0.25 min followed by gradient to 85% acetonitrile/15% water over 1.5 min and continuation of 85% acetonitrile/15% water for 2.25 min with a Luna C18 column (2.1 mm × 50 mm, 3.5 μm) at a flow rate of 1.25 mL/min. Elemental analysis was performed by Atlantic Microlabs (Norcross, GA). All final compounds biologically tested were confirmed to be of >95% purity by the HPLC methods described above. All animal studies were conducted according to protocols approved by the Johns Hopkins University Animal Care and Use Committee.

5,6-Dimethyl-4-(*o*-tolyloxy)thieno[2,3-*d*]pyrimidine (1a).

To a solution of *o*-cresol (0.41 g, 3.78 mmol) in DMF (8 mL) at 0 °C was added NaH (60% w/w, 0.15 g, 3.78 mmol). After the mixture was stirred at 0 °C for 10 min, 4-chloro-5,6-dimethylthieno[2,3-*d*]pyrimidine **2a** (0.50 g, 2.52 mmol) was added in one portion as a solid. The reaction was stirred at 0 °C and was gradually warmed up to rt and stirred overnight. After ice water was added to quench the reaction, the mixture was concentrated and taken up in Et_2O (40 mL). The mixture was washed with H_2O (20 mL) and brine (20 mL), dried over Na_2SO_4, and concentrated. The resulting solid residue was triturated with EtOAc/hexanes (1:4) to afford 0.4 g of the desired product as a white solid (59% yield); mp 106–108 °C. ^{1}H NMR ($CDCl_3$) δ 2.20 (s, 3H), 2.53 (s, 3H). 2.59 (s, 3H), 7.15 (dd, J = 1.0 Hz, J = 7.6 Hz, 1H), 7.23 (m, 1H), 7.32 (m, 2H), 8.48 (s, 1H); ^{13}C NMR ($CDCl_3$) δ 13.6, 13.8, 16.5, 119.9,

122.2, 125.1, 126.0, 127.1, 130.6, 131.4, 132.6, 150.8, 152.2, 163.0, 167.7. LCMS: t_R 2.23 min, *m/z* 271 $[M + H]^+$.

4-(*o*-Tolyloxy)thieno[2,3-*d*]pyrimidine (1b).

Compound **1b** was prepared as described for the preparation of **1a** except 4-chlorothieno[2,3-*d*]pyrimidine **2b** was used in place of 4-chloro-5,6-dimethylthieno[2,3-*d*]pyrimidine **2a**. White solid (82% yield); mp 63–64 °C. ^{1}H NMR ($CDCl_3$) δ 2.18 (s, 3H), 7.12–7.39 (m, 4H), 7.49–7.60 (m, 2H), 8.61 (s, 1H); ^{13}C NMR ($CDCl_3$) δ 16.3, 118.5, 118.9, 122.0, 125.5, 126.3, 127.2, 130.6, 131.5, 150.7, 153.4, 163.4, 169.5. LCMS: t_R 1.98 min, *m/z* 243 $[M + H]^+$.

5,6-Dimethyl-4-phenoxythieno[2,3-*d*]pyrimidine (1c).

Compound **1c** was prepared as described for the preparation of **1a** except phenol was used in place of *o*-cresol. White solid (67% yield); mp 107–109 °C. ^{1}H NMR ($CDCl_3$) δ 2.51 (s, 3H), 2.56 (s, 3H), 7.20–7.33 (m, 3H), 7.44–7.51 (m, 2H), 8.49 (s, 1H); ^{13}C NMR ($CDCl_3$) δ 13.5, 13.6, 120.1, 121.8, 125.0, 125.6, 129.6, 132.6, 151.9, 152.2, 163.1, 167.7. LCMS: t_R 2.16 min, *m/z* 257 $[M + H]^+$.

5,6-Dimethyl-4-(*m*-tolyloxy)thieno[2,3-*d*]pyrimidine (1d).

Compound **1d** was prepared as described for the preparation of **1a** except *m*-cresol was used in place of *o*-cresol. White solid (44% yield); mp 154–155 °C. ^{1}H NMR ($CDCl_3$) δ 2.41 (s, 3H), 2.51 (s, 3H), 2.55 (s, 3H), 6.99–7.07 (m, 2H), 7.11 (d, J = 7.6 Hz, 1H), 7.35 (t, J = 7.7 Hz, 1H), 8.50 (s, 1H); ^{13}C NMR ($CDCl_3$) δ 13.6, 13.7, 21.4, 118.8, 120.2, 122.4, 125.1, 126.6, 129.4, 132.6, 140.0, 152.1, 152.3, 163.3, 167.8. LCMS: t_R 2.29 min, *m/z* 271 $[M + H]^+$.

5,6-Dimethyl-4-(*p*-tolyloxy)thieno[2,3-*d*]pyrimidine (1e).

Compound **1e** was prepared as described for the preparation of **1a** except *p*-cresol was used in place of *o*-cresol. White powder (50% yield); mp 90–94 °C. ^{1}H NMR ($CDCl_3$) δ 2.40 (s, 3H), 2.50 (s, 3H), 2.56 (s, 3H), 7.11 (d, J = 8.4 Hz, 2H), 7.26 (d, J = 8.4 Hz, 2H), 8.49 (s, 1H); ^{13}C NMR ($CDCl_3$) δ 13.5, 13.6, 20.9, 120.1, 121.50, 121.52, 125.1, 130.19, 130.21, 132.5, 135.3, 150.0, 152.01, 152.03, 163.4, 167.6. LCMS: t_R 2.26 min, *m/z* 271 $[M + H]^+$.

4-(2-Fluorophenoxy)-5,6-dimethylthieno[2,3-*d*]pyrimidine (1f).

Compound **1f** was prepared as described for the preparation of **1a** except 2-fluorophenol was used in place of *o*-cresol. White powder (75% yield); mp 143–145 °C. ^{1}H NMR ($CDCl_3$) δ 2.53 (s, 3H), 2.59 (s, 3H), 7.22–7.39 (m, 4H), 8.50 (s, 1H); ^{13}C NMR ($CDCl_3$) δ 13.57, 13.62, 116.8 (d, J_{CF} = 18.3 Hz), 119.8, 124.0, 124.6 (d, J_{CF} = 4 Hz), 125.0, 127.0 (d, J_{CF} = 7 Hz), 133.0, 139.6 (d, J_{CF} = 12.7 Hz), 151.77, 151.82, 154.5 (d, J_{CF} = 249 Hz), 162.3, 167.9. LCMS: t_R 2.22 min, *m/z* 275 $[M + H]^+$.

4-(3-Fluorophenoxy)-5,6-dimethylthieno[2,3-*d*]pyrimidine (1g).

Compound **1g** was prepared as described for the preparation of **1a** except 3-fluorophenol was used in place of *o*-cresol. White solid (62% yield); mp 158–161 °C. ^{1}H NMR ($CDCl_3$)

δ 2.51 (s, 3H), 2.53–2.56 (m, 5H), 6.96–7.07 (m, 5H), 7.38–7.47 (m, 1H), 8.50 (s, 1H); ^{13}C NMR ($CDCl_3$) δ 13.6, 109.9 (d, J_{CF} = 24.2 Hz), 112.7 (d, J_{CF} = 20.9 Hz), 117.6 (d, J_{CF} = 3.4 Hz), 120.1, 124.9, 130.4 (d, J_{CF} = 9.3 Hz), 133.2, 151.8, 153.2 (d, J_{CF} = 10.8 Hz), 162.6, 163.1 (d, J_{CF} = 248 Hz), 168.0. LCMS: t_R 2.16 min, *m/z* 275 $[M + H]^+$.

4-(4-Fluorophenoxy)-5,6-dimethylthieno[2,3-*d*]pyrimidine (1h).

Compound **1h** was prepared as described for the preparation of **1a** except 4-fluorophenol was used in place of *o*-cresol. White fluffy needles (54% yield); mp 137–140 °C. ^{1}H NMR ($CDCl_3$) δ 2.51 (s, 3H), 2.55 (s, 3H), 7.12–7.22 (m, 5H), 8.48 (s, 1H); ^{13}C NMR ($CDCl_3$) δ 13.6, 13.7, 116.3 (d, J_{CF} = 23.6 Hz), 120.0, 123.3 (d, J_{CF} = 8.3 Hz), 125.0, 132.9, 148.0 (d, J_{CF} = 3 Hz), 151.8, 160.1 (d, J_{CF} = 244 Hz), 163.1, 167.8. LCMS: t_R 2.16 min, *m/z* 275 $[M + H]^+$.

5,6-Dimethyl-4-(2-(trifluoromethyl)phenoxy)thieno[2,3-*d*]pyrimidine (1i).

Compound **1i** was prepared as described for the preparation of **1a** except 2-(trifluoromethyl)phenol was used in place of *o*-cresol. White powder (53% yield). mp 155–157 °C. ^{1}H NMR ($CDCl_3$) δ 2.52 (s, 3H), 2.55 (s, 3H), 7.34–7.45 (m, 2H), 7.64–7.70 (m, 1H), 7.77 (d, J = 7.9 Hz, 1H), 8.47 (s, 1H). ^{13}C NMR ($CDCl_3$) δ 13.3, 13.7, 120.0, 123.0 (q, J_{CF} = 273 Hz), 123.4, 124.7, 125.1, 125.7, 127.2 (q, J_{CF} = 4.8 Hz), 133.0, 133.2, 149.65, 151.6, 162.5, 168.1. LCMS: t_R 2.29 min, *m/z* 325 $[M + H]^+$.

5,6-Dimethyl-4-(3-(trifluoromethyl)phenoxy)thieno[2,3-*d*]pyrimidine (1j).

Compound **1j** was prepared as described for the preparation of **1a** except 3-(trifluoromethyl)phenol was used in place of *o*-cresol. White solid (71% yield); mp 120–126 °C. ^{1}H NMR ($CDCl_3$) δ 2.52 (s, 3H), 2.56 (s, 3H), 7.40–7.65 (m, 4H), 8.49 (s, 1H); ^{13}C NMR ($CDCl_3$) δ 13.6, 119.1 (q, J_{CF} = 3.8 Hz), 120.1, 122.4 (q, J_{CF} = 3.9 Hz), 123.5 (q, J_{CF} = 272 Hz) 124.8, 125.5, 130.1, 132.1 (q, J_{CF} = 32.9 Hz), 133.3, 151.6, 152.4, 162.5, 168.1. LCMS: t_R 2.38 min, *m/z* 325 $[M + H]^+$.

5,6-Dimethyl-4-(4-(trifluoromethyl)phenoxy)thieno[2,3-*d*]pyrimidine (1k).

Compound **1k** was prepared as described for the preparation of **1a** except 4-(trifluoromethyl)phenol was used in place of *o*-cresol. Light yellow needles (33% yield). mp 115–120 °C. ^{1}H NMR ($CDCl_3$) δ 2.52 (s, 3H), 2.55 (s, 3H), 7.36 (d, 2H), 7.73 (d, 2H), 8.49 (s, 1H). ^{13}C NMR ($CDCl_3$) δ 13.62, 13.65, 120.2, 122.2, 123.9 (q, J_{CF} = 271 Hz), 124.8, 127.0 (q, J_{CF} = 3.7 Hz), 127.8 (q, J_{CF} = 32.9 Hz), 133.4, 151.66, 151.70, 154.9, 162.4, 168.2. LCMS: t_R 2.35 min, *m/z* 325 $[M + H]^+$.

4-(2-Fluorophenoxy)thieno[2,3-*d*]pyrimidine (1l).

Compound **1l** was prepared as described for the preparation of **1a** except 2-fluorophenol was used in place of *o*-cresol, and 4-chlorothieno[2,3-*d*]pyrimidine **2b** was used in place of 4-chloro-5,6-dimethylthieno[2,3-*d*]pyrimidine **2a**. White solid (36% yield). mp 104–106 °C. ^{1}H NMR ($CDCl_3$) δ 7.20–7.37 (m, 4H), 7.53 (d, J = 5.9 Hz, 1H), 7.57 (dd, J = 6.0, 0.6 Hz, 1H), 8.62 (s, 1H). ^{13}C NMR ($CDCl_3$) δ 116.9 (d, $J_{C\text{-}F}$ = 18.3 Hz), 117.0, 118.4, 118.7,

123.9, 124.8 (d, J_{CF} = 3.7 Hz), 125.9, 127.2 (d, J_{CF} = 7.1 Hz), 139.4 (d, J_{CF} = 12.6 Hz), 153.1, 154.4 (d, J_{CF} = 250 Hz), 162.8, 169.7. LCMS: t_R 1.92 min, *m/z* 247 $[M + H]^+$.

4-(2-Fluorophenoxy)-5-methylthieno[2,3-*d*]pyrimidine (1m).

Compound **1m** was prepared as described for the preparation of **1a** except 2-fluorophenol was used in place of *o*-cresol, and 4-chloro-5-methylthieno[2,3-d]pyrimidine **2c** was used in place of 4-chloro-5,6-dimethylthieno[2,3-*d*]pyrimidine **2a**. Beige fluffy solid (93% yield). mp 98–102 °C. ^{1}H NMR ($CDCl_3$) δ 2.69 (s, 3H), 7.09 (s, 1H), 7.19–7.38 (m, 4H), 8.55 (s, 1H). ^{13}C NMR ($CDCl_3$) δ 17.0, 116.9 (d, J_{CF} = 18.3 Hz), 118.6, 120.6, 124.0, 124.7 (d, J_{CF} = 3.9 Hz), 127.1 (d, J_{CF} = 6.9 Hz), 130.5, 139.5 (d, J_{CF} = 12.6 Hz), 152.9, 154.5 (d, J_{CF} = 249 Hz), 163.6, 170.4. LCMS: t_R 2.07 min, *m/z* 261 $[M + H]^+$.

4-(2-Fluorophenoxy)-6-methylthieno[2,3-*d*]pyrimidine (1n).

Compound **1n** was prepared as described for the preparation of **1a** except 2-fluorophenol was used in place of *o*-cresol, and 4-chloro-6-methylthieno[2,3-*d*]pyrimidine **2d** was used in place of 4-chloro-5,6-dimethylthieno[2,3-*d*]pyrimidine **2a**. White solid (84% yield). mp 135–138 °C. ^{1}H NMR ($CDCl_3$) δ 2.67 (s, 3H), 7.19–7.37 (m, 5H), 8.55 (s, 1H). ^{13}C NMR ($CDCl_3$) δ 16.4, 115.5, 116.9 (d, J_{CF} = 18.5 Hz), 119.5, 123.9, 124.7 (d, J_{CF} = 3.9 Hz), 127.1 (d, J_{CF} = 7 Hz), 139.5 (d, J_{CF} = 12.5 Hz), 140.8, 152.2, 154.4 (d, J_{CF} = 250 Hz), 161.5, 169.5. LCMS: t_R 2.07 min, *m/z* 261 $[M + H]^+$.

4-(2-Fluorophenoxy)-5-(trifluoromethyl)thieno[2,3-*d*]pyrimidine (1o).

Compound **1o** was prepared as described for the preparation of **1a** except 2-fluorophenol was used in place of *o*-cresol, and 4-chloro-5-(trifluoromethyl)thieno[2,3-*d*]pyrimidine **2e**[16] was used in place of 4-chloro-5,6-dimethylthieno[2,3-*d*]pyrimidine **2a**. White cake solid (90% yield). mp 65–66 °C. ^{1}H NMR ($CDCl_3$) δ 7.22 – 7.27 (m, 2H), 7.28 – 7.34 (m, 2H), 8.03 (s, 1H), 8.67 (s, 1H). ^{13}C NMR ($CDCl_3$) δ 114.4, 117.0 (d, J_{CF} = 18.2 Hz), 121.1 (q, J_{CF} = 270 Hz), 123.2 (q, J_{CF} = 38 Hz), 123.7, 124.8 (d, J_{CF} = 4.1 Hz), 127.5 (d, J_{CF} = 7 Hz), 128.4 (q, J_{CF} = 5.9 Hz), 139.2 (d, J_{CF} = 12.7 Hz), 154.2, 154.3 (d, J_{CF} = 250 Hz), 162.3, 170.3. LCMS: t_R 2.13 min, *m/z* 315 $[M + H]^+$.

6-(*tert*-butyl)-4-(2-fluorophenoxy)thieno[2,3-*d*]pyrimidine (1p).

Compound **1p** was prepared as described for the preparation of **1a** except 2-fluorophenol was used in place of *o*-cresol, and 6-(*tert*-butyl)-4-chlorothieno[2,3-*d*]pyrimidine **2f** was used in place of 4-chloro-5,6-dimethylthieno[2,3-*d*]pyrimidine **2a**. Clear oil (60% yield). ^{1}H NMR ($CDCl_3$) δ 1.51 (s, 9H), 7.21–7.35 (m, 5H), 8.54 (s, 1H). ^{13}C NMR ($CDCl_3$) δ 32.0, 35.4, 111.7, 116.9 (d, J_{CF} = 18.3 Hz), 119.1, 123.9, 124.8 (d, J_{CF} = 3.8 Hz), 127.1 (d, J_{CF} = 7.2 Hz), 139.6 (d, J_{CF} = 12.6 Hz), 152.3, 154.5 (d, J_{CF} = 250 Hz), 158.1, 161.8, 169.0. LCMS: t_R 2.41 min, *m/z* 303 $[M + H]^+$.

6-*tert*-butyl-5-phenylthieno[2,3-*d*]pyrimidin-4-ol (4).

In a vial, 3,3-dimethyl-1-phenylbutan-1-one **3** (500 mg, 2.84 mmol), ethylcyanoacetate (483 mg, 4.26 mmol), sulfur (726 mg, 2.84 mmol), formamide (0.9 mL, 22.7 mmol), L-proline (65.3 mg, 0.57 mmol), and diethylamine (41.5 mg, 0.57 mmol) was heated to 170 °C and

stirred for 6 h. After the vial cooled to rt, the residue was triturated with DCM. The resulting black solid was removed by filtration and the filtrate was concentrated and purified by Biotage Isolera One, using 30–50% EtOAc in DCM as eluent to give 35 mg of the desired compound as yellow solid (4% yield). ^{1}H NMR ($CDCl_3$) δ 1.24 (s, 9H), 7.25–7.31 (m, 2H), 7.34–7.46 (m, 3H), 10.91 (s, 1H). LCMS: t_R 1.98 min, *m/z* 285 $[M + H]^+$.

6-*tert*-butyl-4-chloro-5-phenylthieno[2,3-*d*]pyrimidine (5).

A solution of **4** (35 mg, 0.12 mmol) in $POCl_3$ (0.5 mL) was stirred at 110 °C for 1 h. Excess $POCl_3$ was removed in vacuo followed by co-evaporation with DCM, three times. The crude was purified by Biotage Isolera One using 0–10% EtOAc in DCM as eluent to give 25 mg of the desired compound as yellow oil (66% yield). ^{1}H NMR ($CDCl_3$) δ 1.30 (s, 9H), 7.28–7.32 (m, 2H), 7.38–7.47 (m, 3H), 8.76 (s, 1H). LCMS: t_R 2.44 min, *m/z* 303 $[M + H]^+$.

6-*tert*-butyl-4-(2-fluorophenoxy)-5-phenylthieno[2,3-*d*]pyrimidine (1q).

Sodium hydride (60% dispersion in mineral oil, 5.3 mg, 0.13 mmol) was added to a solution of 2-fluorophenol (14.8 mg, 0.13 mmol) in DMF (0.2 mL) at 0 °C and the mixture was stirred at 0 °C for 5–10 min. A solution of **5** (20 mg, 0.07 mmol) in DMF (0.3 mL) was then added slowly to the mixture via syringe at 0 °C. The reaction mixture was stirred and allowed to warm to rt overnight. A few drops of 10% $KHSO_4$ were added to the mixture to quench the excess NaH and the mixture was then concentrated in vacuo. The crude residue was triturated in methanol and water to give 10 mg of desired compound as a light yellow solid (40% yield); Mp 81–82 °C. ^{1}H NMR ($CDCl_3$) δ 1.33 (s, 9H), 6.92 (dt, J = 8.4, 4.1 Hz, 1H), 7.03–7.17 (m, 3H), 7.27–7.44 (m, 5H), 8.50 (s, 1H); ^{13}C NMR ($CDCl_3$) δ 32.6, 36.4, 116.6 (d, J_{CF} =18 Hz), 123.5, 124.4, 126.6 (d, J_{CF} = 7 Hz), 127.4, 127.5, 129.1, 130.4, 137.1, 143.0 (d, J_{CF} = 19 Hz), 151.0, 152.2, 154.1 (d, J_{CF} = 250 Hz), 162.2, 165.9. LCMS: t_R 2.64 min, *m/z* 379 $[M + H]^+$.

6-*tert*-Butyl-4-methoxythieno[2,3-*d*]pyrimidine (6).

To a solution of 6-*tert*-butyl-4-chlorothieno[2,3-*d*]pyrimidine **2f** (1.62 g, 7.15 mmol) in methanol (20 mL) at 0 °C was added 25 wt. % sodium methoxide in methanol (17.2 mmol, 3.92 mL). The mixture was stirred at 0 °C for 30 min, then at rt for 1 h. The solvent was removed in vacuo and water was carefully added to quench excess of sodium methoxide. The compound was extracted with EtOAc and the organic layer was dried over Na_2SO_4 and concentrated to give 1.56 g of the desired compound as a yellow oil which was used without further purification (98% crude yield). ^{1}H NMR ($CDCl_3$) δ 1.45 (s, 9H), 4.12 (s, 3H), 7.06 (s, 1H), 8.59 (s, 1H).

5-Bromo-6-*tert*-butyl-4-methoxythieno[2,3-*d*]pyrimidine (7).

To a solution of **6** (1.56 g, 7.02 mmol) in AcOH (30 mL) was added N-bromosuccinimide (3.75 g, 21.1 mmol) and the mixture was stirred at 55 °C overnight. The reaction was concentrated and the crude material was purified by Biotage Isolera One using 0–10% EtOAc in hexanes as eluent to give 1.8 g of the desired compound as a light-yellow solid (85% yield). ^{1}H NMR ($CDCl_3$) δ 1.59 (s, 9H), 4.14 (s, 3H), 8.59 (s, 1H).

6-(*tert*-butyl)-5-(4-fluorophenyl)-4-methoxythieno[2,3-*d*]pyrimidine (8a).

A suspension of **7** (200 mg, 0.66 mmol), 4-fluorophenylboronic acid (186 mg, 1.33 mmol), potassium carbonate (4.13 g, 29.9 mmol), and bis(triphenylphosphine)palladium(II) dichloride (46.6 mg, 0.07 mmol) in DMF (8 mL) was purged with N_2 gas via an inserted long needle for 30 min. The mixture was then stirred at 80 °C overnight. After removing solvent in vacuo, water was added to the mixture. The mixture was extracted with dichloromethane twice and the combined extracts were washed with brine, dried over Na_2SO_4, and concentrated. The resulting white precipitate was removed by filtration and the filtrate was concentrated and purified by Biotage Isolera One using 5% EtOAc/DCM as eluent to give 190 mg of the desired compound as a thick brown oil (92% yield). ^{1}H NMR ($CDCl_3$) δ 1.27 (s, 9H), 3.69 (s, 3H), 7.02 – 7.12 (m, 2H), 7.19 – 7.26 (m, 2H), 8.56 (s, 1H).

6-*tert*-Butyl-5-(3,4-dichlorophenyl)-4-methoxythieno[2,3-*d*]pyrimidine (8b).

A suspension of **7** (3.00 g, 9.96 mmol), 3,4-dichlorophenylboronic acid (3.80 g, 19.9 mmol), potassium carbonate (4.13 g, 29.9 mmol), and bis(triphenylphosphine)palladium(II) dichloride (0.699 g, 1.00 mmol) in DMF (45 mL) was purged with N_2 gas via an inserted long needle for 30 min. The mixture was then stirred at 80 °C overnight. After removing solvent in vacuo, water was added to the mixture. The mixture was extracted with dichloromethane twice and the combined extracts were washed with brine, dried over Na_2SO_4, and concentrated. The resulting white precipitate was removed by filtration and the filtrate was concentrated and purified by Biotage Isolera One using 5% EtOAc/DCM as eluent to give 2.73 g of the desired compound as a thick brown oil (75% yield). ^{1}H NMR ($CDCl_3$) δ 1.30 (s, 9H), 3.74 (s, 3H), 7.13 (dd, J = 2.0, 8.1 Hz, 1H), 7.40 (d, J = 2.0 Hz, 1H), 7.45 (d, J = 8.3 Hz, 1H), 8.58 (s, 1H).

6-*tert*-Butyl-5-(4-fluorophenyl)thieno[2,3-*d*]pyrimidin-4-ol (9a).

To a solution of **8a** (189 mg, 0.60 mmol) in DCM (6 mL) at 0 °C was added 1 M BBr_3 solution in DCM (1.80 mL, 1.80 mmol). The mixture was stirred at 0 °C, then gradually warmed to rt and stirred until completion (overnight). The mixture was then cooled to 0 °C and methanol was added to quench excess of BBr_3. After removal of solvents, the crude material was partitioned between water and dichloromethane. The organic layer was washed with brine, dried over Na_2SO_4, and concentrated. The residual solid was purified by Biotage Isolera One using 20–35% EtOAc in hexanes with 2% AcOH as eluent to give 75 mg of the desired compound as a white solid (41% yield). ^{1}H NMR ($CDCl_3$) δ 1.25 (s, 9H), 7.05 – 7.12 (m, 2H), 7.22 – 7.27 (m, 2H), 7.77 (s, 1H), 10.59 (s, 1H).

6-*tert*-Butyl-5-(3,4-dichlorophenyl)thieno[2,3-*d*]pyrimidin-4-ol (9b).

To a solution of **8b** (1.50 g, 4.08 mmol) in DCM (50 mL) at 0 °C was added 1 M BBr_3 solution in DCM (20.4 mL, 20.4 mmol). The mixture was stirred at 0 °C, then gradually warmed to rt and stirred until completion (7 days). The mixture was then cooled to 0 °C and methanol was added to quench excess of BBr_3. After removal of solvents, the crude material was partitioned between water and dichloromethane. The organic layer was washed with brine, dried over Na_2SO_4, and concentrated. The residual solid was triturated with dichloromethane to give 1.27 g of the desired compound as a white solid (93% yield). ^{1}H

NMR ($CDCl_3$) δ 1.28 (s, 9H), 7.14 (dd, J = 2.0, 8.1 Hz, 1H), 7.40 (d, J = 2.0 Hz, 1H), 7.46 (d, J = 8.3 Hz, 1H), 7.76 (s, 1H), 11.25 (s, 1H).

6-*tert*-Butyl-4-chloro-5-(4-fluorophenyl)thieno[2,3-*d*]pyrimidine (10a).

A solution of **9a** (70 mg, 0.23 mmol) in $POCl_3$ (3 mL) was stirred at 110 °C for 1 h. Excess $POCl_3$ was removed in vacuo followed by co-evaporation with DCM (three times). The residual material was passed through a short silica column using 5% EtOAc in hexanes as eluent to give 45 mg of the desired compound as a yellow solid (61% yield). ^{1}H NMR ($CDCl_3$) δ 1.30 (s, 9H), 7.08 – 7.18 (m, 2H), 7.24 – 7.34 (m, 2H), 8.77 (s, 1H).

6-*tert*-Butyl-4-chloro-5-(3,4-dichlorophenyl)thieno[2,3-*d*]pyrimidine (10b).

A solution of **9b** (2.00 g, 5.66 mmol) in $POCl_3$ (15 mL) was stirred at 110 °C for 1 h. Excess $POCl_3$ was removed in vacuo followed by co-evaporation with DCM (three times). The residual material was passed through a short silica column using 0–10% EtOAc in DCM as eluent to give 2.00 g of the desired compound as a white solid (95% yield). ^{1}H NMR ($CDCl_3$) δ 1.33 (s, 9H), 7.17 (dd, J = 2.0, 8.3 Hz, 1H), 7.45 (d, J = 2.0 Hz, 1H), 7.51 (d, J = 8.1 Hz, 1H), 7.79 (s, 1H).

6-(*tert*-butyl)-4-(2-fluorophenoxy)-5-(4-fluorophenyl)thieno[2,3-*d*]pyrimidine (1r).

To a solution of 2-fluorophenol (41.9 mg, 0.37 mmol) in DMF (1 mL) was added sodium hydride (60 % dispersion in mineral oil, 11.2 mg, 0.28 mmol) at 0 °C and the mixture was stirred at 0 °C for 5–10 min. A solution of **10a** (60 mg, 0.19 mmol) in DMF (2 mL) was then slowly added to the mixture via syringe at 0 °C. The reaction mixture was gradually warmed up to rt and stirred overnight. A few drops of 10% $KHSO_4$ was added to the mixture to quench excess of NaH and the mixture was concentrated in vacuo. The crude material was partitioned between water and EtOAc. The organic layer was washed with brine, dried over sodium sulfate, and concentrated. The residual material was purified by Biotage Isolera One using 10% EtOAc in hexanes as eluent to give 60 mg of desired compound as a light tan solid (77% yield); mp 172–173 °C. ^{1}H NMR ($CDCl_3$) δ 1.33 (s, 9H), 6.94 (t, J = 8.0 Hz, 1H), 7.01 – 7.22 (m, 5H), 7.32 – 7.43 (m, 2H), 8.51 (s, 1H); ^{13}C NMR ($CDCl_3$) δ 32.6, 36.4, 114.5 (d, J_{CF} = 21 Hz), 116.7 (d, J_{CF} = 18 Hz), 120.4, 123.6, 124.4 (d, J_{CF} = 4 Hz), 126.7 (d, J_{CF} = 6.8 Hz), 127.9, 132.0 (d, J_{CF} = 8.1 Hz), 133.0 (d, J_{CF} = 3.5 Hz), 139.3 (d, J_{CF} = 12.7 Hz), 151.6, 152.4, 154.1 (d, J_{CF} = 249 Hz), 162.2, 162.3 (d, J_{CF} = 247 Hz), 165.9. LCMS: t_R 2.63 min, m/z 397 $[M + H]^+$.

6-(*tert*-butyl)-5-(4-fluorophenyl)-4-(2-(trifluoromethoxy)phenoxy)thieno[2,3-*d*]pyrimidine (1s).

To a solution of 2-trifluoromethoxyphenol (35 mg, 0.31 mmol) in DMF (1 mL) was added sodium hydride (60 % dispersion in mineral oil, 12.5 mg, 0.31 mmol) at 0 °C and the mixture was stirred at 0 °C for 5–10 min. A solution of **10b** (50 mg, 0.16 mmol) in DMF (1 mL) was then slowly added to the mixture via syringe at 0 °C. The reaction mixture was gradually warmed up to rt and stirred overnight. A few drops of 10% $KHSO_4$ was added to the mixture to quench excess of NaH and the mixture was concentrated in vacuo. The crude material was partitioned between water and EtOAc. The organic layer was washed

with brine, dried over sodium sulfate, and concentrated. The residual material was purified by Biotage Isolera One using 0–10% EtOAc in hexanes as eluent to give 46 mg of desired compound as a yellow solid (65% yield); mp 127–129 °C. ^{1}H NMR ($CDCl_3$) δ 1.33 (s, 9H), 6.98 – 7.07 (m, 3H), 7.22 – 7.38 (m, 5H), 8.49 (s, 1H); ^{13}C NMR ($CDCl_3$) δ 29.6, 32.5, 36.4, 114.5 (d, J_{CF} = 21.5 Hz), 120.2 (q, J_{CF} = 259 Hz) 120.3, 122.3, 122.7, 124.0, 124.4, 126.5, 126.8, 127.6, 127.8, 127.9, 132.0 (d, J_{CF} = 8.1 Hz), 132.8 (d, J_{CF} = 3.7 Hz), 140.87, 140.90, 143.8, 151.7, 152.2, 152.4, 162.2, 162.3 (d, J_{CF} = 246 Hz) 165.9. LCMS: t_R 2.63 min, *m/z* 463 $[M + H]^+$.

6-*tert*-butyl-5-(3,4-dichlorophenyl)-4-(2-(trifluoromethoxy)phenoxy)thieno[2,3-*d*]pyrimidine (1t).

To a solution of 2-trifluoromethoxyphenol (0.529 g, 2.97 mmol) in DMF (6 mL) was added sodium hydride (60 % dispersion in mineral oil, 0.119 g, 2.97 mmol) at 0 °C and the mixture was stirred at 0 °C for 5–10 min. A solution of **10b** (0.920 g, 2.48 mmol) in DMF (15 mL) was then slowly added to the mixture via syringe at 0 °C. The reaction mixture was gradually warmed up to rt and stirred overnight. A few drops of 10% $KHSO_4$ was added to the mixture to quench excess of NaH and the mixture was concentrated in vacuo. The crude material was partitioned between water and EtOAc. The organic layer was washed with brine, dried over sodium sulfate, and concentrated. The residual material was purified by Biotage Isolera One using $CHCl_3$ as eluent to give 0.880 g of desired compound as a white solid (69% yield); mp 85–89 °C. ^{1}H NMR ($CDCl_3$) δ 1.35 (s, 9H), 7.02 (m, 1H), 7.23–7.33 (m, 4H), 7.43 (d, J = 8.3 Hz, 1H), 7.51 (d, J = 2.0 Hz, 1H), 8.51 (s, 1H); ^{13}C NMR ($CDCl_3$) δ 32.6, 36.5, 119.9, 120.2 (q, J_{CF} = 259 Hz), 122.4, 124.1, 126.2, 126.7, 127.7, 129.5, 129.9, 131.6, 131.8, 132.2, 137.0, 140.9, 143.7, 152.3, 152.4, 162.1, 166.0. LCMS: t_R 2.98 min, *m/z* 513.1 $[M + H]^+$. Anal. Calcd. for $C_{23}H_{17}Cl_2F_3N_2O_2S$: C, 53.81; H, 3.34; N, 5.46; S, 6.25; F, 11.10; Cl, 13.81. Found: C, 53.82; H, 3.41; N, 5.38, S, 6.23; F, 10.93; Cl, 13.87.

In vitro MRGPRX1 receptor assay.

HEK293 cells stably transfected with human *MrgprX1* were plated in 96 well plates at 25,000 cell /well and incubated 2 days before imaging. On the day of imaging cells were incubated in 100 μL HBSS with 2 μM Fluo 4AM and 1% Trypan Red for 50 minutes at 37°C. The cells were then equilibrated for 10 minutes at room temperature before imaging. Test compounds were dissolved in HBSS and diluted in a serial dilution. Test compounds, BAM 8–22 (positive control) or HBSS (negative control) were added (50 μL into 100 μL) and cells were imaged on the FLIPR for 2 minutes. Data was exported as maximum – minimum fluorescent signal.

In vitro Metabolic Stability Studies.

The metabolic stability was evaluated using mouse and human liver microsomes as previously reported.[17] The assay was carried out with 100 mM potassium phosphate buffer, pH 7.4, in the presence of NADPH regenerating system (1.3 mM NADPH, 3.3 mM glucose 6-phosphate, 3.3 mM $MgCl_2$, 0.4 U/mL glucose-6-phosphate dehydrogenase, 50 μM sodium citrate). Reactions, in triplicate, were initiated by addition of the liver microsomes to the incubation mixture (compound final concentration was 5 μM; 0.5 mg/mL microsomes).

Controls in the absence of cofactors were carried out to determine the specific cofactor-free degradation. After 30 and 60 min of incubation, aliquots of the mixture were removed in triplicate and the reaction quenched by addition of three times the volume of ice-cold acetonitrile spiked with the internal standard. Compound disappearance was monitored over time using a liquid chromatography and tandem mass spectrometry (LC/MS/MS) method.

Metabolite identification studies.

Metabolite identification was performed on samples obtained from human liver microsomes. Samples (2 μL) were injected on an Agilent 1290 UPLC coupled to an Agilent 6520 quadrupole time of flight mass spectrometer. Metabolites were separated on an Agilent Eclipse Plus C18 1.8 μm, 2.1 × 100 mm column with a 5-minute gradient from 97.5/2.5 to 5/95 water + 0.1% formic acid/acetonitrile + 0.1% formic acid mobile phase. Analysis was performed in positive ion mode, with fragmentation by collision induced dissociation with a collision energy set at 25. Product ions were identified using MassHunter Qualitative analysis software.

In vivo pharmacokinetic studies in mice.

All pharmacokinetic studies in mice were conducted according to protocols approved by the Animal Care and Use Committee at Johns Hopkins University. Male CD 1 mice between 25 and 30 g were obtained from Harlan, Inc., and maintained on a 12-hour light-dark cycle with *ad libitum* access to food and water. Compound **1t** was given to mice (n=3) by oral gavage at 100 mg/kg in a vehicle (5% dimethyl acetamide, 10% Cremophor EL, 10% Tween80, 25% PEG400, and 50% water). The mice were sacrificed at predetermined time points (0.25–6 h) post drug administration. For collection of plasma and spinal cord and brain, animals were euthanized with CO_2, and blood samples were collected in heparinized microtubes by cardiac puncture. Spinal cords and brains were dissected and immediately flash frozen (−80 °C). Plasma was obtained by centrifugation of blood at 3,000 *g* for 15 minutes, and stored at −80 °C until LC/MS analysis.

Prior to extraction, frozen samples were thawed on ice. The calibration curves were developed using plasma and spinal cord from naïve animals as a matrix. Plasma samples (50 μL), were processed using a single liquid extraction method by addition of 300 μL of acetonitrile as with internal standard (losartan [5 μM]), followed by vortexing for 30 s and then centrifugation at 10000 rcf for 10 min. For spinal cord tissue, homogenized samples were vortexed and centrifuged as above. A 10 μL aliquot of supernatant was diluted with 40 μL water containing 0.5 μM losartan as internal standard. Extracts were centrifuged at 10000 rcf at 4 °C for 10 minutes. Supernatants were transferred to 250 μL polypropylene autosampler vials sealed with a Teflon cap. A volume of 3 μL was injected onto the ultra-performance liquid chromatography (UPLC) instrument for quantitative analysis by LC/MS/MS. Calibration curves over the 0.01–10 nmol/mL plasma and spinal cord were constructed from the peak area ratio of the analyte to the internal standard using linear regression with a weighting factor of 1/(nominal concentration). Correlation coefficient of greater than 0.99 was obtained in all analytical runs for all analytes.

Sciatic nerve chronic constrictive injury (CCI) model of neuropathic pain.

MRGPRX1 mice were generated as described in our previous study.[8] MRGPRX1 mice (both sexes) were bred at the Johns Hopkins University, and had access *ad libitum* to food and water. Neuropathic pain was induced by CCI surgery to the sciatic nerve in adult mice (2- to 3-month-old, 20–30 g). Mice were anesthetized by inhalation of 2% isoflurane delivered through a nose cone. Skin was shaved, and small incision was made at the level of the mid-thigh. The left sciatic nerve was exposed by blunt dissection through the biceps femoris, and separated from the surrounding tissue. The nerve trunk proximal to the distal branching point was loosely tied with three nylon sutures (6–0 nonabsorbable braided silk suture, 18020–60, Fine Science Tools, CA, USA) until the epineurium was slightly compressed and minor twitching of the relevant muscles was observed. The ligatures were approximately 0.5 mm apart. The muscle layer was closed with 4–0 silk suture and the wound closed with suture.

Supplementary Material

Refer to Web version on PubMed Central for supplementary material.

ACKNOWLEDGMENT

This research was supported by NIH grants UG3NS115718 (T.T.), R21NS101954 (TT), R01NS054791 (XD), R01NS070814 (Y.G.), R01NS117761 (Y.G.), R01NS110598 (Y.G.), 5T32NS070201 (I.B.), and the Johns Hopkins Institute for Clinical and Translational Research (ICTR), which is funded in part by UL1TR001079 from the National Center for Advancing Translational Sciences (NCATS). XD is an investigator of the Howard Hughes Medical Institute. Animal behavioral studies were facilitated by the Pain Research Core funded by the Blaustein Fund and the Neurosurgery Pain Research Institute at the Johns Hopkins University.

ABBREVIATIONS

MRGPRX1	mas-related G-protein coupled receptor member X1
DRG	dorsal root ganglion
HTS	high throughput screening
CCI	chronic constriction injury

REFERENCES

1. Dong X; Han S; Zylka MJ; Simon MI; Anderson DJ A diverse family of gpcrs expressed in specific subsets of nociceptive sensory neurons. Cell 2001, 106, 619–632. [PubMed: 11551509]
2. Lembo PM; Grazzini E; Groblewski T; O'Donnell D; Roy MO; Zhang J; Hoffert C; Cao J; Schmidt R; Pelletier M; Labarre M; Gosselin M; Fortin Y; Banville D; Shen SH; Strom P; Payza K; Dray A; Walker P; Ahmad S Proenkephalin a gene products activate a new family of sensory neuron--specific gpcrs. Nat Neurosci 2002, 5, 201–209. [PubMed: 11850634]
3. Chen H; Ikeda SR Modulation of ion channels and synaptic transmission by a human sensory neuron-specific g-protein-coupled receptor, snsr4/mrgx1, heterologously expressed in cultured rat neurons. J Neurosci 2004, 24, 5044–5053. [PubMed: 15163697]
4. Li Z; He SQ; Xu Q; Yang F; Tiwari V; Liu Q; Tang Z; Han L; Chu YX; Wang Y; Hin N; Tsukamoto T; Slusher B; Guan X; Wei F; Raja SN; Dong X; Guan Y Activation of mrgc receptor inhibits n-type calcium channels in small-diameter primary sensory neurons in mice. Pain 2014, 155, 1613–1621. [PubMed: 24813294]

5. Wilson SR; Gerhold KA; Bifolck-Fisher A; Liu Q; Patel KN; Dong X; Bautista DM Trpa1 is required for histamine-independent, mas-related g protein-coupled receptor-mediated itch. Nat Neurosci 2011, 14, 595–602. [PubMed: 21460831]
6. Wroblowski B; Wigglesworth MJ; Szekeres PG; Smith GD; Rahman SS; Nicholson NH; Muir AI; Hall A; Heer JP; Garland SL; Coates WJ The discovery of a selective, small molecule agonist for the mas-related gene x1 receptor. J. Med. Chem 2009, 52, 818–825. [PubMed: 19146417]
7. Prchalova E; Hin N; Thomas AG; Veeravalli V; Ng J; Alt J; Rais R; Rojas C; Li Z; Hihara H; Aoki M; Yoshizawa K; Nishioka T; Suzuki S; Kopajtic T; Chatrath S; Liu Q; Dong X; Slusher BS; Tsukamoto T Discovery of benzamidine- and 1-aminoisoquinoline-based human mas-related g-protein-coupled receptor x1 (mrgprx1) agonists. J Med Chem 2019, 62, 8631–8641. [PubMed: 31498617]
8. Li Z; Tseng PY; Tiwari V; Xu Q; He SQ; Wang Y; Zheng Q; Han L; Wu Z; Blobaum AL; Cui Y; Tiwari V; Sun S; Cheng Y; Huang-Lionnet JH; Geng Y; Xiao B; Peng J; Hopkins C; Raja SN; Guan Y; Dong X Targeting human mas-related g protein-coupled receptor x1 to inhibit persistent pain. Proc Natl Acad Sci U S A 2017, 114, E1996–E2005. [PubMed: 28223516]
9. Wen W; Wang Y; Li Z; Tseng PY; McManus OB; Wu M; Li M; Lindsley CW; Dong X; Hopkins CR Discovery and characterization of 2-(cyclopropanesulfonamido)-n-(2-ethoxyphenyl)benzamide, ml382: A potent and selective positive allosteric modulator of mrgx1. ChemMedChem 2015, 10, 57–61. [PubMed: 25209672]
10. Woszczek G; Fuerst E Ca2+ mobilization assays in gpcr drug discovery. Methods Mol Biol 2015, 1272, 79–89. [PubMed: 25563178]
11. Shi T; Kaneko L; Sandino M; Busse R; Zhang M; Mason D; Machulis J; Ambrose AJ; Zhang DD; Chapman E One-step synthesis of thieno[2,3-d]pyrimidin-4(3h)-ones via a catalytic four-component reaction of ketones, ethyl cyanoacetate, s8 and formamide. ACS Sustain Chem Eng 2019, 7, 1524–1528. [PubMed: 31754553]
12. Pubchem identifier: Aid 602413. https://pubchem.ncbi.nlm.nih.gov/bioassay/602413
13. McNeil BD; Pundir P; Meeker S; Han L; Undem BJ; Kulka M; Dong X Identification of a mast-cell-specific receptor crucial for pseudo-allergic drug reactions. Nature 2015, 519, 237–241. [PubMed: 25517090]
14. Bowes J; Brown AJ; Hamon J; Jarolimek W; Sridhar A; Waldron G; Whitebread S Reducing safety-related drug attrition: The use of in vitro pharmacological profiling. Nat Rev Drug Discov 2012, 11, 909–922. [PubMed: 23197038]
15. Bennett GJ; Xie YK A peripheral mononeuropathy in rat that produces disorders of pain sensation like those seen in man. Pain 1988, 33, 87–107. [PubMed: 2837713]
16. Taylor S; Murfin S; Coulter TS; Jaekel S; Aicher B; Kelter A-R; Krämer J; Kirchhoff C; Scheel A; Wölcke J Thienopyrimidines for pharmaceutical compositions. PCT Int. Appl. WO2006/136402, 2006.
17. Giancola JB; Bonifazi A; Cao J; Ku T; Haraczy AJ; Lam J; Rais R; Coggiano MA; Tanda G; Newman AH Structure-activity relationships for a series of (bis(4-fluorophenyl)methyl)sulfinylethyl-aminopiperidines and -piperidine amines at the dopamine transporter: Bioisosteric replacement of the piperazine improves metabolic stability. Eur J Med Chem 2020, 208, 112674. [PubMed: 32947229]

BAM8-22

Val-Gly-Arg-Pro-Glu-Trp-Trp-Met-Asp-Tyr-Gln-Lys-Arg-Tyr-Gly

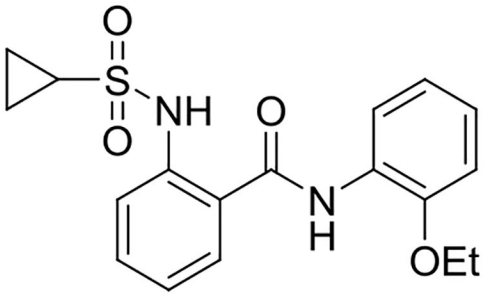

ML382

EC_{50} = 0.19 **μ**M

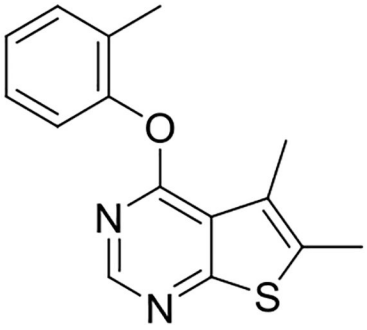

1a

EC_{50} = 0.5 **μ**M

Figure 1.

Chemical structures of BAM8-22, ML382, and compound **1a**.

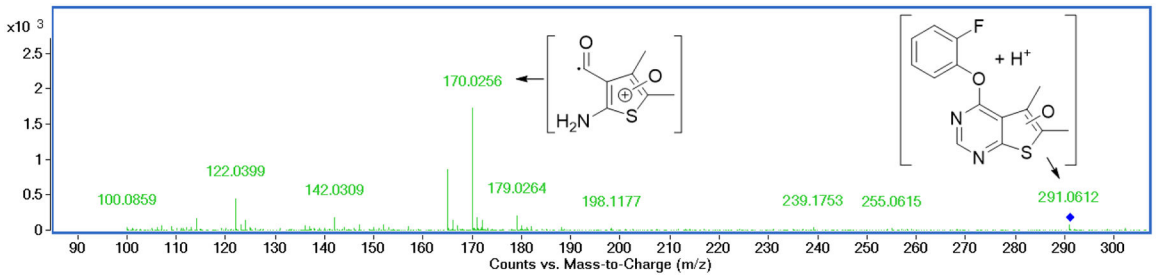

Figure 2.

Identification of the major metabolite of compound **1f** incubated in human liver microsomes. MS/MS spectroscopy of the major metabolite [MH^+ + 16] shows a fragment corresponding to the oxidized thiophenium moiety.

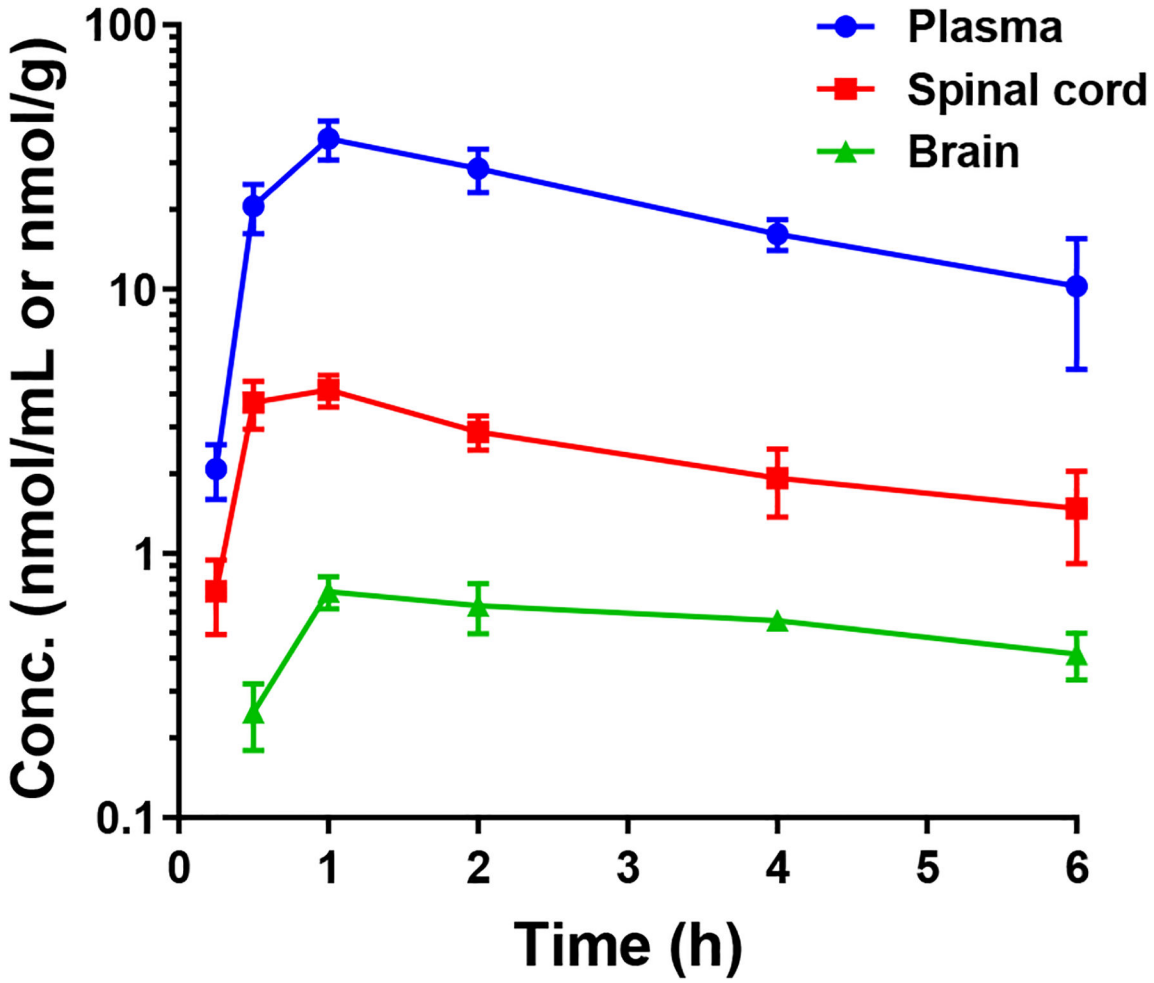

Figure 3.

Plasma, spinal cord, and brain levels of compound **1t** in mice following oral administration (100 mg/kg).

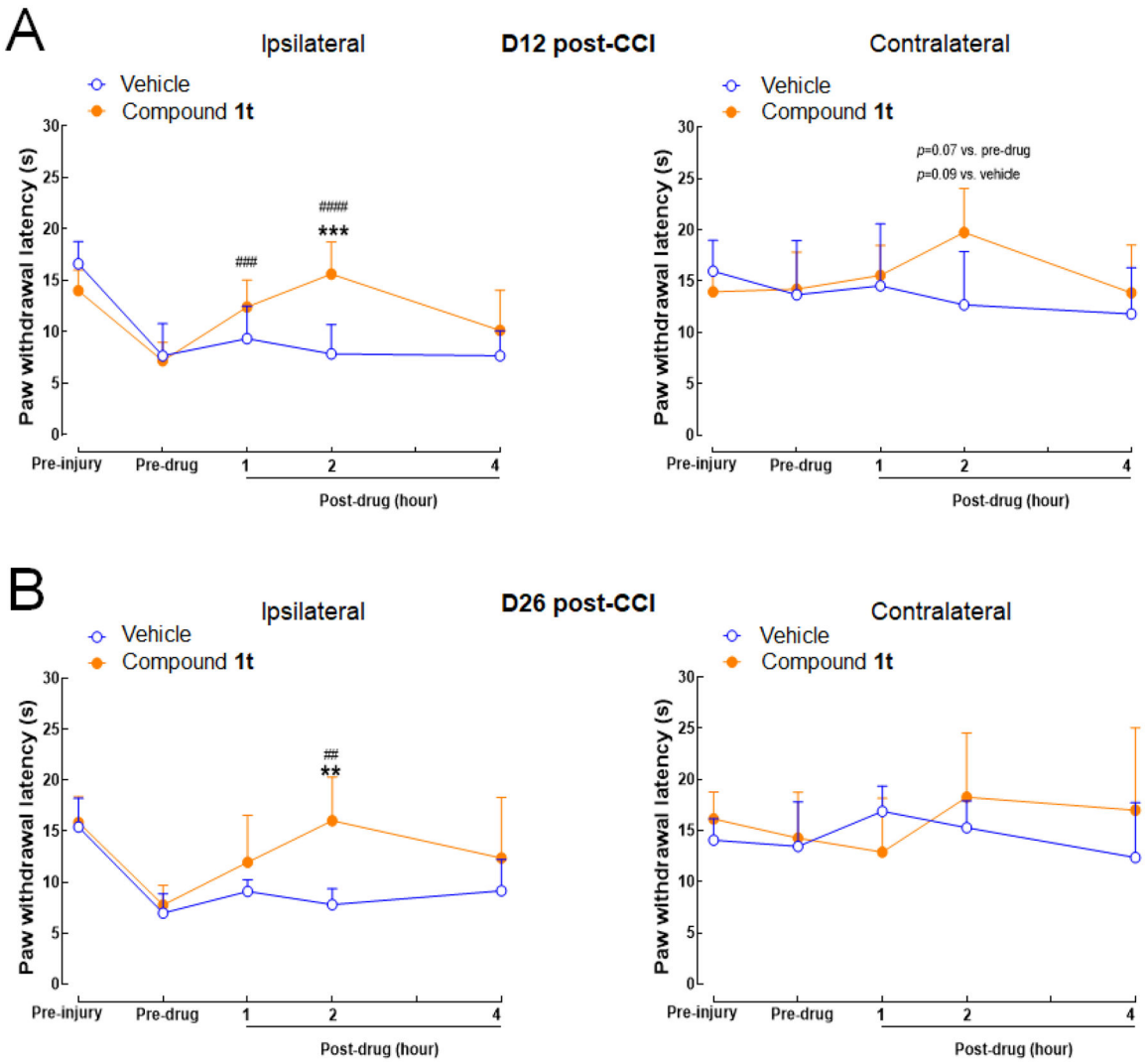

Figure 4.

Oral administration of compound **1t** attenuated heat hypersensitivity in the ipsilateral hind paw of MRGPRX1 mice subjected to sciatic nerve CCI. **(A)** Paw withdrawal latency (PWL) to noxious heat stimuli was measured with the Hargreaves test. PWLs were increased from pre-drug level after treated with compound **1t** (100 mg/kg, po, n=5), but not those treated with vehicle (n=4) on day 12 post-CCI, and (B) on day 26 post-CCI (n=5/group). ** P<0.01, *** P<0.001 vs. vehicle; ## P<0.01, ### P<0.001, #### P<0.0001 vs. pre-drug. Two-way mixed-model ANOVA with Bonferroni post hoc test. Data are expressed as mean + SD.

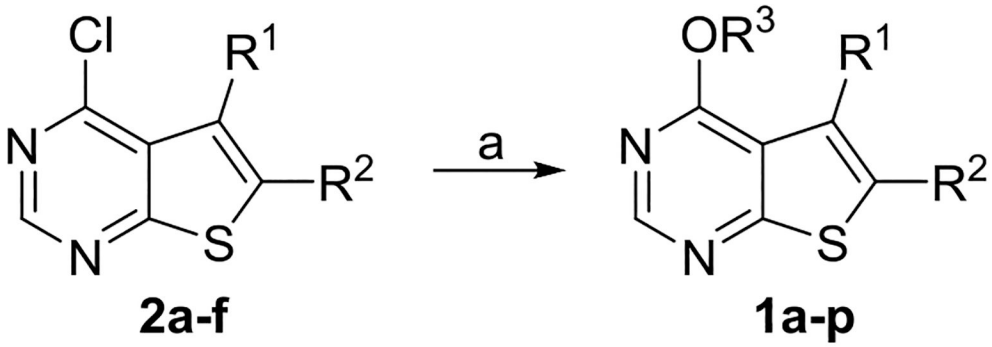

2a-f **1a-p**

R^1 = H, CH_3, or CF_3; R^2 = H, CH_3, or $C(CH_3)_3$;
R^3 = Ph, 2-MePh, 3-MePh, 4-MePh, 2-FPh, 3-FPh, 4-FPh, 2-CF_3Ph, 3-CF_3Ph, or 4-CF_3Ph
The individual molecular structures **1a-p** are shown in Table 1.

Scheme 1.
Synthesis of Compounds **1a-p**[a]
[a]Reagents and conditions: (a) R^3OH, NaH, DMF, 0 °C to rt, 33–93%.

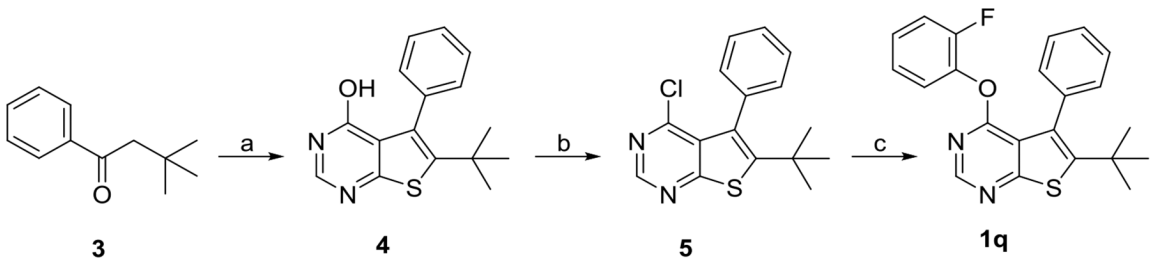

Scheme 2.

Synthesis of Compound **1q**[a]

[a]Reagents and conditions: (a) ethylcyanoacetate, S_8, formamide, L-proline, Et_2NH, 170 °C, 4% (b) $POCl_3$, 100 °C, 66%; (c) 2-fluorophenol, NaH, DMF, 0 °C to rt, 40%.

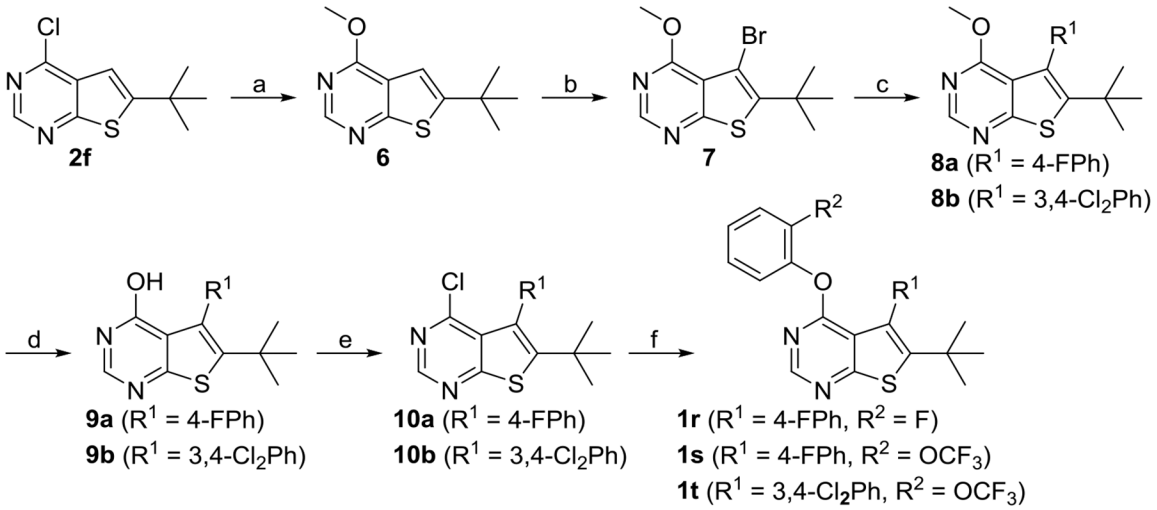

Scheme 3.

Synthesis of Compounds **1r-t**[a]

[a]Reagents and conditions: (a) MeONa, MeOH, 0 °C to rt, 98%; (b) NBS, AcOH, 55 °C, 85%; (c) $R^1B(OH)_2$, $PdCl_2(PPh_3)_2$, K_2CO_3, DMF, 80 °C, 92% for **8a**, 75% for **8b**; (d) BBr_3, DCM, rt, 41% for **9a**, 93% for **9b**; (e) $POCl_3$, 110 °C, 61% for **10a**, 95% for **10b**; (f) 2-fluorophenol or 2-(trifluoromethoxy)phenol, NaH, DMF, 0 °C to rt, 77% for **1r**, 65% for **1s**, 69% for **1t**.

Table 1.

In vitro Potency of Compounds **1a-t** as MRGPRX1 PAMs[a,b]

Cmpd	Structure	EC_{50} (μM)[a] (E_{max})[b]	Cmpd	Structure	EC_{50} (μM)[a] (E_{max})[b]
1a	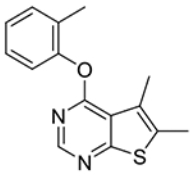	0.48 ± 0.04 (118%)	**1k**	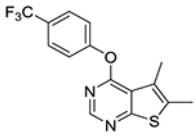	>100
1b	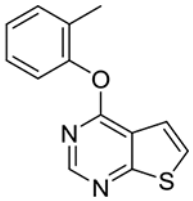	14.5 ± 1.1 (88%)	**1l**	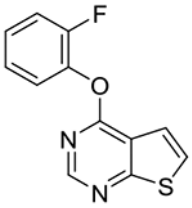	4.2 ± 1.1 (95%)
1c	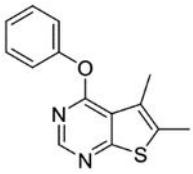	1.6 ± 0.4 (89%)	**1m**	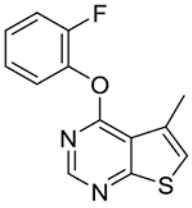	1.7 ± 0.2 (94%)
1d	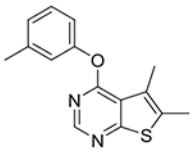	25 (40%)	**1n**	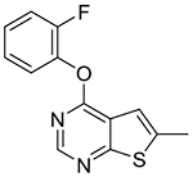	1.5 ± 0.2 (90%)
1e	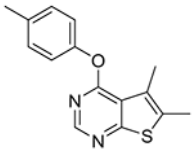	2.7 ± 1.5 (88%)	**1o**	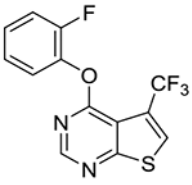	2.1 ± 0.4 (94%)
1f	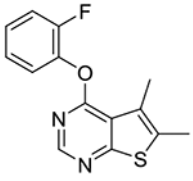	0.22 ± 0.02 (112%)	**1p**	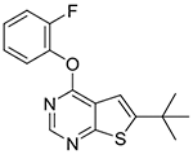	0.32 ± 0.06 (105%)

Cmpd	Structure	EC_{50} (μM)[a] (E_{max})[b]	Cmpd	Structure	EC_{50} (μM)[a] (E_{max})[b]
1g	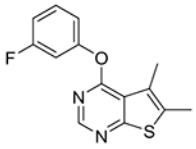	30 (55%)	**1q**	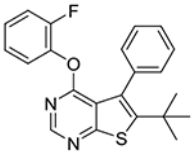	0.34 ± 0.07 (95%)
1h	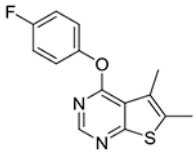	1.1 ± 0.2 (83%)	**1r**	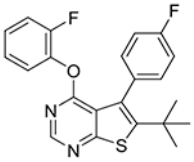	0.30 ± 0.13 (145%)
1i	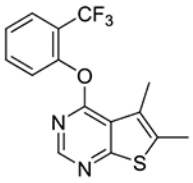	0.52 ± 0.03 (95%)	**1s**	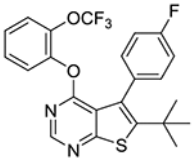	0.23 ± 0.05 (143%)
1j	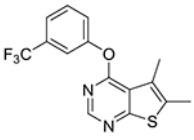	>100	**1t**	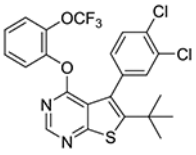	0.10 ± 0.01 (114%)

[a]Values are mean ± standard error of the mean (SEM) of at least three independent experiments performed in quadruplicate.

[b]E_{max} values were defined as response elicited by maximum concentration of test compounds in the presence of EC_{20} concentration of BAM8–22 normalized to that elicited by 250 nM (>EC_{100}) of BAM8–22 alone.

Table 2.

Metabolic Stability in Mouse and Human Liver Microsomes

Cmpd	%remaining			
	Mouse		Human	
	30 min	60 min	30 min	60 min
1f	<5	<5	<5	<5
1o	<5	<5	40	<5
1p	<5	<5	75	61
1q	14	<5	94	78
1r	7	<5	>95	88
1s	28	5	>95	>95
1t	58	25	>95	>95

Table 3.

In Vivo Pharmacokinetic Profiles of Compound **1t**

	T_{max} (h)	C_{max} (nmol/mL or nmol*h/g)	$AUC_{0\text{-}last}$ (nmol*h/mL or nmol*h/g)	Tissue-to-plasma ratio (by AUC)
Plasma	1	38.98 ± 5.06	108.53 ± 1.18	
Brain	1	0.82 ± 0.05	2.37 ± 0.03	2.2%
Spinal cord	1	4.60 ± 0.60	13.79 ± 0.14	12.7%